

Front propagation in a random medium with a power-law distribution of transit times

Jean-Marc Debierre

Laboratoire MATOP, Case 151, Faculté des Sciences et Techniques de Saint-Jérôme, 13397 Marseille Cedex 20, France

R. Mark Bradley

Department of Physics, Colorado State University, Fort Collins, Colorado 80523

(Received 13 June 1994)

We perform Monte Carlo simulations of front propagation in a two-dimensional random medium in which a fraction $1-p$ of the bonds have infinite transit time and the remainder have finite transit times t drawn from a probability distribution $f(t)$. We take $f(t)$ to be zero for $t < 1$ and to decay as $t^{-\tau}$ for $t \geq 1$. At the percolation threshold, we recover the usual values for the kinetic critical exponents when $\tau > 2$, but these exponents vary continuously with τ for $\tau \in (1, 2]$. For $p = 1$, the kinetics of the front appear to be correctly described by the Kardar-Parisi-Zhang equation when $\tau > 2$. In contrast, we find anomalous scaling behavior for $\tau = 1.75$.

PACS number(s): 64.60.Ak, 05.70.Ln, 05.40.+j

I. INTRODUCTION

First-passage percolation (FPP) has been applied to such diverse topics as the propagation of signals through random media, the spread of epidemics, combustion of disordered materials, and forest fires [1–7]. FPP is also closely related to the problem of finding the shortest path between two points in a random medium.

To define FPP, it is convenient to speak of the propagation of a combustion front through a disordered material, but it should be kept in mind that the applications are broader than this language suggests. Consider a regular lattice in which all sites and bonds are initially unburned and the bonds all have length a . Each bond is assigned a transit time t drawn from a random distribution $P(t)$. For a given bond, t is the time that it will take the flame front to travel from one end of the bond to the other. Thus a/t is the velocity of flame propagation for this bond. At time $t=0$, a site is set on fire. The flame front propagates along the bonds containing this site with the prescribed velocities. Behind the front there is burned material, and ahead of it is unburned material. At some point, a second site is set alight by the advancing front. The flame front then begins to propagate along the unburned bonds containing this site. The combustion continues in this fashion for all subsequent times. We assume that when material burns, it is completely consumed, and so it can never be burned again.

Kerstein and Edwards (KE) have studied FPP with a binary distribution of transit times $P(t) = p\delta(t-t_-) + (1-p)\delta(t-t_+)$ [8]. Here $p \in [0, 1]$ is a constant and $t_- \leq t_+$. Physically, t_- (t_+) is the transit time for fast-burning (slow-burning) bonds. This model is a generalization of the much-studied special case in which t_- is nonzero and finite and $t_+ = \infty$. We will refer to this special case as “kinetic percolation,” and it describes combustion of a random mixture of flammable and perfectly flame-resistant materials. There is a phase transition in kinetic percolation at the percolation threshold $p = p_c$ for

bond percolation. For $p < p_c$, the front eventually ceases to propagate, while for $p > p_c$ the burning may never cease. In the latter case, if the front does continue to propagate indefinitely, it does so with a well-defined asymptotic front velocity v . As p tends to p_c from above, $v \sim (p - p_c)^\theta$. In two dimensions (2D), Grassberger [9] has estimated that $\theta = 0.176 \pm 0.006$.

KE also considered FPP with a power-law distribution of transit times. Specifically, they set

$$P(t) = pf(t) + (1-p)\delta(t - \infty), \quad (1.1)$$

where

$$f(t) = \begin{cases} (\tau-1)t^{-\tau}, & \text{for } t \geq 1 \\ 0 & \text{otherwise.} \end{cases} \quad (1.2)$$

Note that the parameter τ must exceed 1 for $f(t)$ to be normalizable. For $\tau > 2$, the distribution $f(t)$ has a finite mean \bar{t} , and we expect that the critical behavior will be the same as in kinetic percolation. In contrast, for $1 < \tau \leq 2$, the mean of $f(t)$ is infinite, and anomalous scaling behavior could occur. Indeed, KE developed an approximate variational theory that yields the anomalous exponent

$$\theta = \theta_0 + \frac{2-\tau}{\tau-1} \quad (1.3)$$

for $1 < \tau < 2$. (θ_0 is defined to be the value of θ for $\tau > 2$).

There is another reason that we expect anomalous scaling behavior for $1 < \tau < 2$. As emphasized by KE, there is a close analogy between the first-passage time and the conductivity in disordered media. This analogy was exploited by KE to obtain a scaling form for the propagation velocity v , and to construct their variational theory for the exponent θ . It has long been known that percolation with a sufficiently broad power-law distribution of resistances has an anomalous conductivity exponent [10]. The analogy of KE would therefore suggest that FPP has anomalous scaling behavior for τ close to 1.

In this paper, we perform simulations of FPP with the distribution of transit times given by Eqs. (1.1) and (1.2). Our results suggest that the exponent θ has a value independent of τ for $\tau > 2$, and that this value is the same as that found for kinetic percolation. For $\tau < 2$, the critical exponents vary continuously with τ . The behavior of θ is in reasonable agreement with the variational theory of KE in this region.

We have also studied the scaling behavior of our model for $p = 1$. In this case, all of the bonds are eventually burned, and there is a rough growing interface between the burned and unburned regions. Growing interfaces have been the subject of intensive study since the seminal work of Kardar, Parisi, and Zhang (KPZ) [11]. KPZ studied the time evolution of a surface with height $h(x, t)$ governed by the nonlinear Langevin equation

$$\frac{\partial h}{\partial t} = \nu \frac{\partial^2 h}{\partial x^2} + \frac{\lambda}{2} \left[\frac{\partial h}{\partial x} \right]^2 + \eta(x, t). \quad (1.4)$$

This equation is now known as the (1+1)-dimensional KPZ equation. KPZ considered the case in which the noise $\eta(x, t)$ has a Gaussian distribution with $\langle \eta(x, t) \rangle = 0$ and

$$\langle \eta(x, t) \eta(x', t') \rangle = 2D \delta(x - x') \delta(t - t'),$$

where D is a constant. For growth in a strip of width L , the interface width w scales as

$$w \sim \begin{cases} L^\alpha & \text{for } t \gg L^z \\ t^\beta & \text{for } t \ll L^z, \end{cases} \quad (1.5)$$

where $z = \alpha/\beta$. The values of the critical exponents are known exactly: KPZ showed that $\alpha = \frac{1}{2}$ and $\beta = \frac{1}{3}$. The exponents satisfy the identity

$$z + \alpha = 2. \quad (1.6)$$

It is believed that the KPZ equation describes the scaling behavior of many lattice growth models, including the Eden model and ballistic deposition [12].

Motivated by experiments that yielded values of α substantially greater than the KPZ value of $\frac{1}{2}$, Zhang considered the behavior of interfaces governed by the KPZ equation with a non-Gaussian, power-law distribution of noise [13]. Specifically, he assumed that at any point in the (1+1)-dimensional space η has a probability density $P(\eta)$ that decays as $1/\eta^{1+\mu}$ for $\eta \geq 1$ and that is zero for $\eta < 1$. He also assumed that the noise is independently distributed at each point. Zhang's simulations yielded values of α and β that vary with μ , at least when μ is not too large. The exponents for the Zhang model are now known exactly [14]. In 1+1 dimensions, the exponents vary continuously with μ for $2 < \mu < 5$, and reduce to the KPZ values for $\mu \geq 5$.

Inspired by Zhang's work, Roux and co-workers [15,16] considered a variant of the Eden model in which there is a randomly distributed waiting time $t \geq 0$ at each site. On the diamond hierarchical lattice, Roux *et al.* [16] demonstrated that if the waiting times have the power-law distribution $f(t)$ given by Eq. (1.2), the exponents α and β are independent of τ for all $\tau > 1$.

The model studied by Roux *et al.* differs trivially from our model with $p = 1$: Their waiting times are assigned to sites, while our transit times reside on bonds. This distinction should be irrelevant. The diamond hierarchical lattice resembles 2D Euclidean lattices in many respects [16,17], and can be thought of as providing a crude renormalization group approximation to a square lattice [18]. The work of Roux *et al.* therefore suggests that in our model, the exponents should take on the same values for all $\tau > 1$. For $\tau > 2$, the mean bond transit time \bar{t} is finite, and we expect α and β to take on their KPZ values. Thus the work on the diamond hierarchical lattice leads us to the speculation that the exponents in our model assume their KPZ values for all $\tau > 1$.

Our simulations for $\tau = 3$ agree with this speculation. For $\tau = 1.75$, however, we find anomalous values for the critical exponents. For example, we find $\alpha = 0.43 \pm 0.01$, which differs markedly from the KPZ value. This small value of α indicates that the interface is unusually smooth for $\tau = 1.75$. To our knowledge, a nonzero value of α that is smaller than the KPZ value $\frac{1}{2}$ has not previously been observed [19]. Our finding indicates that, at least in one respect, the diamond hierarchical lattice differs significantly from a 2D Euclidean lattice.

The paper is organized as follows: In Sec. II, we describe the algorithm used in the simulations. Section III is concerned with the simulations at the percolation threshold, while the results obtained for $p = 1$ are presented in Sec. IV. In Sec. V, the main results obtained in this study are summarized.

II. ALGORITHM

We performed simulations of FPP on a square lattice with the transit time distribution given by Eqs. (1.1) and (1.2). The simulations were carried out on a finite square grid L sites wide and H sites high with periodic boundary conditions in the x direction (Fig. 1). For simplicity, we take the lattice spacing a to be unity. At the beginning of each run, all sites in the base row $y = 0$ were ignited simultaneously. All of the other lattice sites were initially unburnt. This initial condition was chosen because it leads to smaller fluctuations than the initial condition in which a single site is set alight at $t = 0$.

We assigned a transit time to a bond only when one of

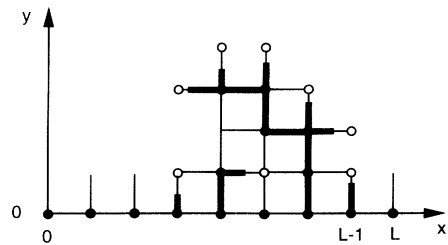


FIG. 1. A schematic representation of the front on a square lattice L sites wide. Periodic boundary conditions are imposed in the x direction, so that the rows at $x = 0$ and L coincide. Bold (thin) lines represent burned (unburned) material. Black (white) dots are burnt (surface) sites.

the sites at its ends started burning. In this way, we avoided assigning transit times to bonds that were never reached by the flame front. At time $t=0$, the state of the bonds was unknown, except for the L vertical bonds connecting the rows $y=0$ and 1.

At any time t , we define the surface of the burned region to be the set of unburnt sites which lie on currently burning bonds. This surface can have both overhangs and disconnected loops (Fig. 1). The surface sites were stored in a list Σ which was ordered according to the times t_B necessary for the front to reach them. Specifically, the first site in the list had the smallest t_B value, and the sites which followed it had successively larger values of t_B . The first site in the list is the first surface site to be burnt, and will be labeled σ .

At each step of the simulation, the following operations were performed sequentially.

(i) Time was incremented by the exact amount δt necessary for the front to reach the site σ .

(ii) The burning times t_B associated with the surface sites were all decreased by δt .

(iii) The site σ was removed from the list Σ .

(iv) Each of the four nearest-neighbor sites of σ was then tested in turn. If a given nearest-neighbor site was still unburnt, the bond connecting it to σ was randomly assigned a transit time t drawn from the distribution $P(t)$. If the site was an additional surface site, it was inserted into list Σ with $t_B=t$. If it was not an additional surface site, the value of t_B for this site was replaced by t if $t < t_B$.

This algorithm was repeated until a given time t_{\max} had elapsed. In practice, the time t_{\max} was chosen so that the top row $y=H$ was never reached by the front, and therefore the grid appeared to be infinite in the vertical direction. The average number N of burnt sites and their mean distance Y from the base row $y=0$ were computed at each time step.

III. RESULTS FOR $p=p_c$

For kinetic percolation with $p=p_c$ on an infinite lattice at large times [3,9],

$$Y \sim t^{\phi_y} \quad (3.1)$$

and

$$N \sim t^{\phi_n} . \quad (3.2)$$

Grassberger has estimated the values of the kinetic critical exponents ϕ_y and ϕ_n using Monte Carlo simulations, and finds $\phi_y=0.883\pm 0.003$ and $\phi_n=0.793\pm 0.004$ [9]. These exponents are related through the scaling relation

$$\phi_n/\phi_y = d_f - 1 , \quad (3.3)$$

where d_f is the fractal dimension of the infinite cluster at threshold [9,20]. The exact value of d_f is $\frac{91}{48}$ [21], and so Grassberger's estimates of ϕ_y and ϕ_n are consistent with Eq. (3.3).

In our model, kinetic percolation is recovered in the limit $\tau \rightarrow \infty$, where the mean bond transit time \bar{t} is equal

to 1. We expect that ϕ_y and ϕ_n will take on their $\tau = \infty$ values for any $\tau > 2$, since \bar{t} is finite in this range. Conversely, \bar{t} diverges for $\tau \in (1, 2]$, and anomalous values of the kinetic critical exponents could occur. The exponents ϕ_y and ϕ_n most likely vary continuously with τ in this interval.

A series of simulations of our model was performed at the bond percolation threshold $p=p_c=\frac{1}{2}$. The simulations were carried out on strips of width L ranging from 1024 to 4096. To compare the data obtained with different strip widths and different τ values, we used a dimensionless time $T=t/t_{\max}$. A log-log plot of Y as a function of T is curved even at $T=1$. As a result, we had to extrapolate our data to the limit $T \rightarrow \infty$. It was also necessary to account for finite-size corrections coming from the finite strip width L . In order to reach both the $1/L \rightarrow 0$ and $1/T \rightarrow 0$ limits, we used the following extrapolation scheme.

(a) log Y was plotted as a function of log T for a given L value. A linear regression was made for all points with $T > T_c$, giving the estimator $\phi_y(L, T_c)$. Extrapolating these estimators to $1/L=0$, we obtained $\phi_y(\infty, T_c)$.

(b) Step (a) was carried out for different times T_c and $\phi_y(\infty, T_c)$ was extrapolated to $1/T_c=0$ to obtain the final estimate for ϕ_y .

A similar procedure was used to extract ϕ_n from the data for $N(t)$. Steps (a) and (b) were carried out with the data obtained for $\tau=1.8$. The results of this two-step extrapolation are displayed in Fig. 2. Our final estimates of the kinetic critical exponents are $\phi_y=0.814\pm 0.004$ and $\phi_n=0.739\pm 0.003$. These exponents are definitely different from their counterparts for kinetic percolation.

Far behind the front, all bonds with finite transit times will have burned. Thus, in this region, the burned sites have the same fractal dimension as the infinite percolation cluster at threshold. For this reason, the scaling relation (3.3) holds for all τ ; the proof runs precisely parallel to that for kinetic percolation [9,20]. With our estimates of ϕ_y and ϕ_n for $\tau=1.8$, we obtain $\phi_n/\phi_y=0.908\pm 0.008$, a value which is slightly too high, but which is nonetheless in satisfactory agreement with the expected result $d_f - 1 = \frac{43}{48} = 0.8958 \dots$

Similar calculations were performed for a number of τ values. However, only two strip widths, $L=1024$ and 4096, were considered for $\tau \neq 1.8$. Instead of extrapolating our data to $1/L \rightarrow 0$, we simply used the results obtained for $L=4096$. The systematic error introduced by this approximation is rather small for $\tau=1.8$ [see Fig. 2(a)]. For $\tau \neq 1.8$, the results obtained for $L=1024$ and 4096 do not differ by much, and so our approximation is reasonably accurate. However, it should be kept in mind that ϕ_y and to a smaller extent ϕ_n are systematically underestimated for $\tau \neq 1.8$. In every case, we extrapolated to $1/T \rightarrow 0$. The resulting estimates of ϕ_y and ϕ_n for τ in the range (1,2) are plotted in Figs. 3 and 4, respectively. Both exponents increase nonlinearly with τ . As $\tau \rightarrow 1$, we expect these exponents to tend to zero, since the probability that the transit time along a bond is less than any finite value vanishes in this limit. On the other hand, the exponents appear to tend to their kinetic percolation

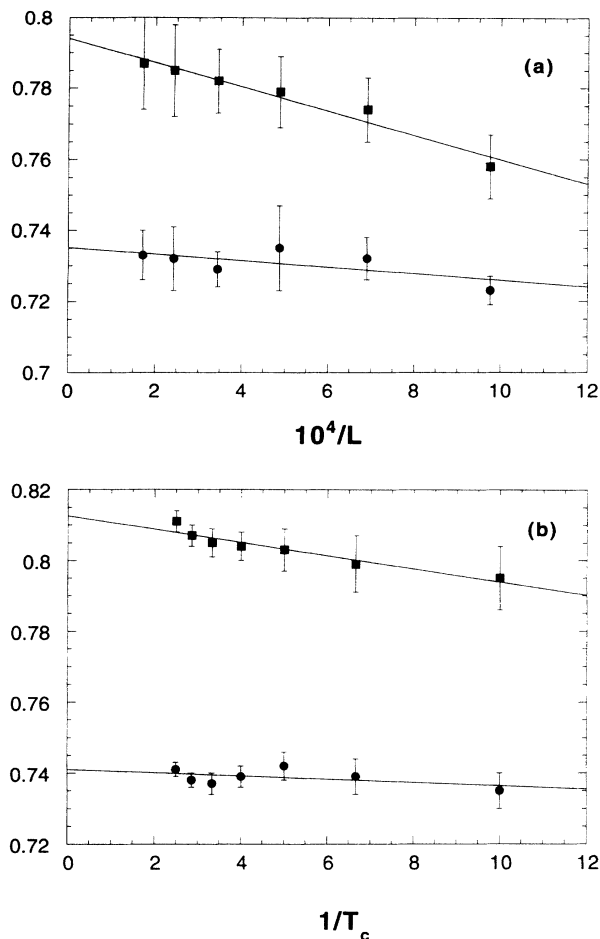


FIG. 2. Two-step extrapolation of the data obtained for $\tau=1.8$ for ϕ_y (■) and ϕ_n (●). (a) Linear extrapolation to $1/L \rightarrow 0$ of the estimates $\phi_y(L, T_c)$ and $\phi_n(L, T_c)$ for $T_c=0.1$. (b) Linear extrapolation to $1/T_c \rightarrow 0$ of the estimates $\phi_y(\infty, T_c)$ and $\phi_n(\infty, T_c)$. The results of this extrapolation give the final estimates for ϕ_y and ϕ_n .

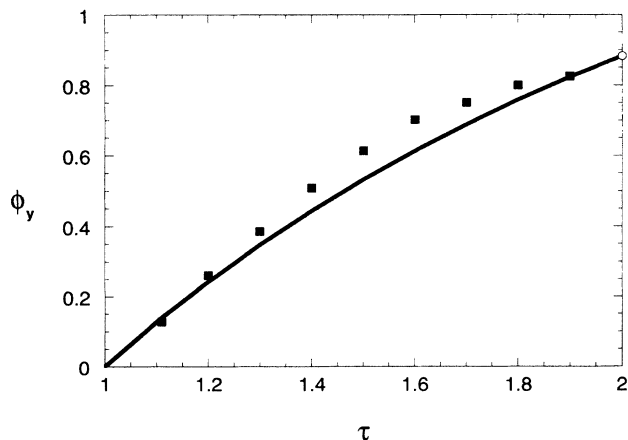


FIG. 3. The kinetic critical exponent ϕ_y (■) as a function of τ . The error bars are comparable in size to the symbols used. The continuous curve shows the prediction of the variational theory of Kerstein and Edwards. The open circle is Grassberger's estimate for ϕ_y for kinetic percolation.

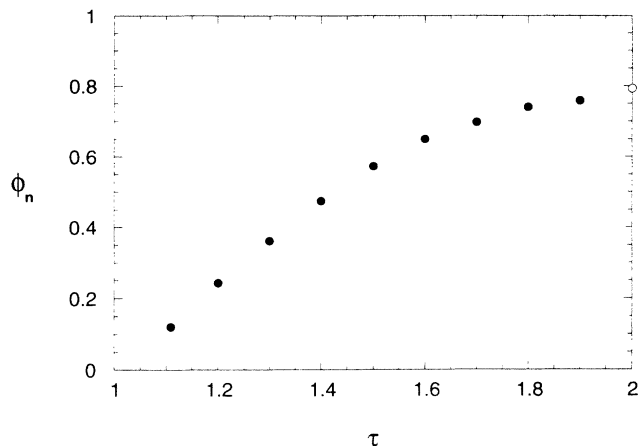


FIG. 4. The kinetic critical exponent ϕ_n (●) as a function of τ . The error bars are comparable in size to the symbols used. The open circle is Grassberger's estimate for ϕ_n for kinetic percolation.

values as $\tau \rightarrow 2$, as expected [22].

Similar calculations for $\tau=3$ and 5 gave $\phi_y=0.873 \pm 0.002$ and $\phi_n=0.795 \pm 0.003$ in both cases. These results are consistent with our belief that the exponents for kinetic percolation should be found for any $\tau > 2$.

A simple scaling argument shows that

$$\frac{1}{\phi_y} = \frac{\theta}{\nu} + 1, \quad (3.4)$$

where ν is the exponent characterizing the divergence of the correlation length. Thus if ϕ_y varies continuously with τ for $1 < \tau < 2$, then so must θ . Moreover, if ϕ_y assumes its kinetic percolation value for $\tau \geq 2$, then so must θ .

The result of KE's variational theory [Eq. (1.3)] can be used to obtain an approximate expression for ϕ_y that applies in the range $1 < \tau < 2$. Let $\phi_{y,0}$ be the value of the exponent ϕ_y that prevails for $\tau > 2$. Combining Eqs. (1.3) and (3.4) and the exact result $\nu = \frac{4}{3}$ [21], we have [23]

$$\frac{1}{\phi_y} = \frac{1}{\phi_{y,0}} + \frac{3}{4} \left[\frac{2-\tau}{\tau-1} \right]. \quad (3.5)$$

This prediction is compared with the results of our simulations in Fig. 3. (Grassberger's value for $\phi_{y,0}$ was used.) The agreement is reasonably good throughout the range of τ values, although the theoretical values for ϕ_y are consistently too small. In fact, as noted by KE, the variational theory overestimates the exponent θ . This means that the variational estimate for ϕ_y should be less than the true value, just as we have found.

IV. RESULTS FOR $p=1$

A series of simulations of our model were carried out on strips of width L for $p=1$. We computed the average height of the surface

$$\bar{y}(t) = \frac{1}{N_s} \sum_{i=1}^{N_s} y_i, \quad (4.1a)$$

as well the surface width

$$w(t) = \left[\frac{1}{N_s} \sum_{i=1}^{N_s} (y_i - \bar{y})^2 \right]^{1/2}. \quad (4.1b)$$

Here N_s is the total number of surface sites and y_i is the y coordinate of the i th surface site. We also calculated the total number $N(t)$ of burnt sites at time t and a characteristic height

$$h(t) \equiv N(t)/L. \quad (4.2)$$

Since h is to a good approximation proportional to t for all but the earliest times, Eq. (1.5) may be rewritten

$$w \sim \begin{cases} L^\alpha & \text{for } h \gg L^z \\ h^\beta & \text{for } h \ll L^z. \end{cases} \quad (4.3)$$

It seemed likely to us that the exponents α and β would take on their KPZ values for $\tau > 2$. However, we also expected anomalous scaling to occur for $1 < \tau < 2$. We performed simulations for $\tau = 1.75$ and 3 to test these beliefs. To determine the exponents α and β , we performed simulations in two distinct limits: $h \gg L^z$ and $h \ll L^z$.

A. The case $h \gg L^z$

In this case, the simulations were performed on relatively narrow strips. The strip width was varied from $L=4$ to 128 and the data were averaged over 1000–16000 independent runs for each L value. Figure 5 is a log-log plot of the front width w as a function of time t for our two different τ values. At sufficiently large times, w saturates at a constant value w_L . The w_L estimates increase as L^α , as shown in Fig. 6. Linear least-squares fits to the data for $L > 16$ give

$$\alpha = \begin{cases} 0.43 \pm 0.01 & \text{for } \tau = 1.75 \\ 0.493 \pm 0.003 & \text{for } \tau = 3. \end{cases} \quad (4.4)$$

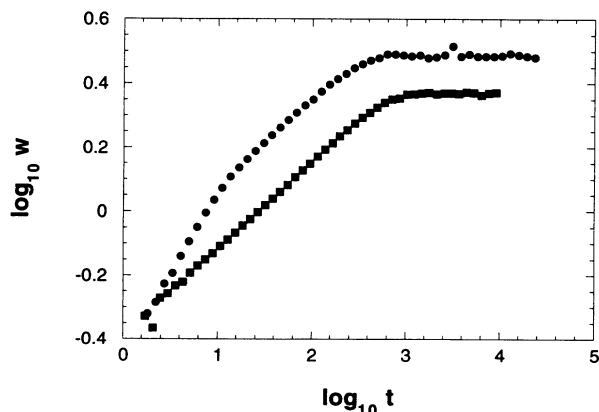


FIG. 5. Log-log plots of the front width w as a function of the time t . The data for $\tau = 1.75$ (●) and 3 (■) were both computed on a strip of width $L = 91$ and were averaged over 1400 samples each.

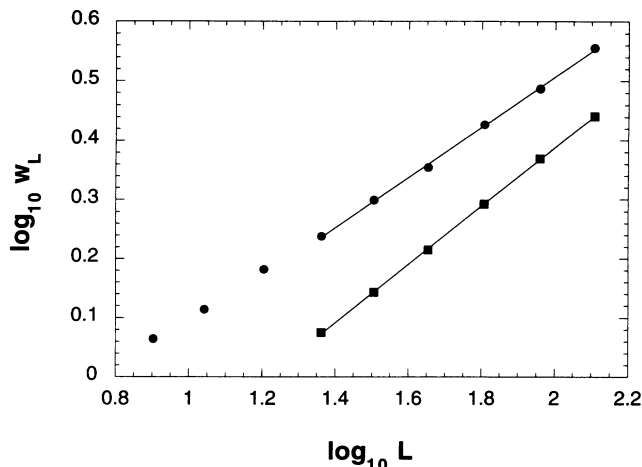


FIG. 6. Log-log plots of the saturation width w_L as a function of the strip width L for $\tau = 1.75$ (●) and 3 (■). The straight lines are linear regressions through the data points. The slopes of these lines give the exponent β for these two τ values.

B. The case $h \ll L^z$

Wider strips were used here, and the number of independent runs varied from 4000 for $L = 512$ to 240 for $L = 8192$. The front width w_i and the characteristic height h_i were computed at 50 different times t_i ($i = 1, 2, \dots, 50$). The log-log plots of w_i as a function of h_i are definitely not linear. To extract the asymptotic behavior of these data, we used the estimator

$$\beta_i = \frac{\log(w_{i+1}/w_{i-1})}{\log(h_{i+1}/h_{i-1})} \quad (4.5)$$

for the exponent β . We assumed that β_i is a linear function of $1/h_i$ at long times (Fig. 7) and then extrapolated to the limit $1/h_i \rightarrow 0$. The resulting estimates of β depend on L , and β_L will denote the estimate for the strip width L . The variations of β_L with $1/L$ are displayed in Fig. 8. Although the scatter of the data points is not negligible, the assumption of linear behavior seems reasonable. Linear extrapolation to $1/L \rightarrow 0$ gave

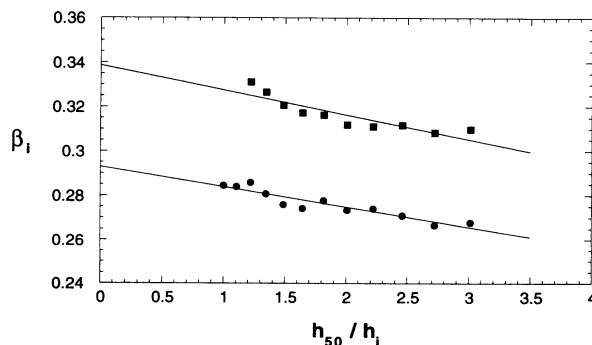


FIG. 7. β_i vs h_{50}/h_i for $\tau = 1.75$ (●) and 3 (■). The strip width L was 4096 in both cases. The lines are least-squares fits to the data points, and the intercepts give β_L .

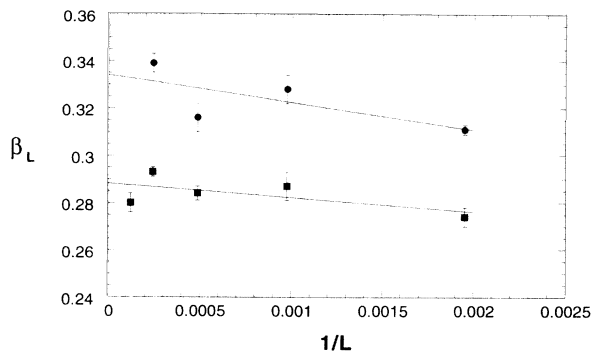


FIG. 8. β_L vs $1/L$ for $\tau=1.75$ (■) and 3 (●). The error bars represent one standard deviation, and the lines are least-squares fits to the data points.

$$\beta = 0.288 \pm 0.002 \quad \text{for } \tau = 1.75. \quad (4.6)$$

Combining this result with our estimate of α [Eq. (4.4)], we obtain

$$z = \alpha/\beta = 1.49 \pm 0.05 \quad \text{for } \tau = 1.75. \quad (4.7)$$

Similarly, we found

$$\beta = 0.334 \pm 0.004 \quad \text{for } \tau = 3 \quad (4.8)$$

and

$$z = \alpha/\beta = 1.48 \pm 0.01 \quad \text{for } \tau = 3. \quad (4.9)$$

Our results strongly suggest that the exponents α and β take on their KPZ values for $\tau=3$. We believe that the exponents have constant values for all $\tau > 2$, since the mean bond transit time $\bar{\tau}$ is finite in this regime. On the other hand, our estimates of the exponents α and β for $\tau=1.75$ differ significantly from the KPZ values $\frac{1}{2}$ and $\frac{1}{3}$. Thus we find anomalous scaling for $\tau=1.75$, contrary to the speculation made in Sec. I. This indicates that the di-

among hierarchical lattice may not be as good a representation of a 2D Euclidean lattice as is sometimes supposed.

It seems likely that α and β vary continuously with τ for $\tau \in (1, 2]$. To test this, calculations would be necessary for τ values between 1 and 2 other than 1.75. Unfortunately, the saturation regime for w shifts to much longer times when τ is decreased, so that the computing time would have to be dramatically increased. On the other hand, as τ tends to 2, the exponents should tend to their KPZ values. As a result, data for $\tau > 1.75$ would have to be averaged over a greater number of samples, since it would be necessary to estimate the exponents with greater accuracy. For both $\tau > 1.75$ and $\tau < 1.75$, the computing power needed exceeds that currently available to us.

V. CONCLUSIONS

In this paper, we performed Monte Carlo simulations of front propagation in a 2D random medium in which a fraction $1-p$ of the bonds have infinite transit time and the remainder have finite transit times drawn from a power-law distribution. At the percolation threshold $p=p_c$, our results indicate that the kinetic critical exponents assume their usual values for $\tau > 2$. In contrast, these exponents vary continuously with τ for $\tau \in (1, 2]$. Our results are in reasonable agreement with the approximate variational theory of Kerstein and Edwards in this regime. For $p=1$, all of the bonds have finite transit times. The kinetics of the front appear to be correctly described by the Kardar-Parisi-Zhang equation when $\tau=3$. We expect the same asymptotic behavior for all $\tau > 2$, since the mean bond transit time is finite in this regime. On the other hand, we find anomalous scaling behavior for $\tau=1.75$. It seems likely that the kinetic critical exponents vary continuously with τ for $1 < \tau < 2$.

ACKNOWLEDGMENTS

We would like to thank J. Amar and K. Wu for helpful discussions. This work was supported in part by NSF Grant No. DMR-9100257.

-
- [1] J. M. Hammersley and D. J. A. Welsh, *Contemp. Phys.* **21**, 593 (1980).
 [2] A. L. Ritzenberg and R. J. Cohen, *Phys. Rev. B* **30**, 4038 (1984).
 [3] P. Grassberger, *Math. Biosci.* **63**, 157 (1983).
 [4] J. L. Cardy and P. Grassberger, *J. Phys. A* **18**, L267 (1985).
 [5] G. MacKay and N. Jan, *J. Phys. A* **17**, L757 (1984).
 [6] G. Albinet, G. Searby, and D. Stauffer, *J. Phys. (France)* **47**, 1 (1986).
 [7] K. Wu and R. M. Bradley, *Phys. Rev. A* **45**, 1255 (1992).
 [8] A. R. Kerstein and B. F. Edwards, *Phys. Rev. B* **33**, 3353 (1986).
 [9] P. Grassberger, *J. Phys. A* **18**, L215 (1985).
 [10] P. M. Kogut and J. P. Straley, *J. Phys. C* **12**, 2151 (1979); A. Ben-Mizrahi and D. J. Bergman, *ibid.* **14**, 909 (1981); P. N. Sen, J. N. Roberts, and B. I. Halperin, *Phys. Rev. B* **32**, 3306 (1985).
 [11] M. Kardar, G. Parisi, and Y. C. Zhang, *Phys. Rev. Lett.* **56**, 889 (1986).
 [12] For example, see T. Vicsek, *Fractal Growth Phenomena* (World Scientific, Singapore, 1989).
 [13] Y.-C. Zhang, *J. Phys. (France)* **51**, 2129 (1990).
 [14] C.-H. Lam and L. M. Sander, *Phys. Rev. Lett.* **69**, 3338 (1992); *Phys. Rev. E* **48**, 979 (1993).
 [15] S. Roux, A. Hansen, and E. L. Hinrichsen, *J. Phys. A* **24**, L295 (1991).
 [16] S. Roux, A. Hansen, L. R. da Silva, L. S. Lucena, and R.

- B. Pandey, *J. Stat. Phys.* **65**, 183 (1991).
- [17] T. Halpin-Healy, *Phys. Rev. Lett.* **63**, 917 (1989); *Phys. Rev. A* **42**, 711 (1990).
- [18] A. N. Berker and S. Ostland, *J. Phys. C* **12**, 4961 (1979); M. Kaufman and R. B. Griffiths, *Phys. Rev. B* **24**, 496 (1981); **30**, 244 (1984).
- [19] The interface width diverges logarithmically with L in kinetic roughening of Laplacian fronts [J. Krug and P. Meakin, *Phys. Rev. Lett.* **66**, 703 (1991)].
- [20] S. Havlin and R. Nossal, *J. Phys. A* **17**, L427 (1984).
- [21] D. Stauffer and A. Aharony, *Introduction to Percolation Theory* (Taylor and Francis, London, 1992).
- [22] Actually, our estimates for ϕ_y and ϕ_n tend to values slightly smaller than Grassberger's as $\tau \rightarrow 2^-$. We believe that if an extrapolation to $1/L \rightarrow 0$ were made for each value of τ , this small discrepancy would disappear.
- [23] This result can also be derived using a "links-nodes-blobs" theory [R. M. Bradley and J.-M. Debierre (unpublished)].